

Fracture properties of a rigid polyurethane foam over a range of densities

A. McIntyre and G. E. Anderton

Department of Polymer Technology, John Dalton Faculty of Technology, Manchester Polytechnic, Manchester M1 5GD

(Received 29 June 1978; revised 19 October 1978)

Single edge notch fracture tests have been carried out on rigid polyurethane foam in the density range 32 to 360 kg/m³. Fracture properties were characterized in terms of the fracture toughness parameter (K_{Ic}), the critical strain energy release rate (G_{Ic}) and crack opening displacement (c.o.d.). The values of crack opening displacement lead to a proposed mechanism of crack propagation in foams of density greater than about 140 kg/m³.

INTRODUCTION

With the increased use of rigid urethane foam in building applications and the feasibility of it being used in load bearing applications it is important to assess carefully the strength of the material and the parameters which determine it. Linear elastic fracture mechanics (l.e.f.m.) have frequently been used to describe the fracture properties of brittle materials¹⁻³ and in this article the concepts of l.e.f.m. have been applied to rigid urethane foam to estimate values of fracture toughness.

The major physical parameter determining the mechanical properties of a rigid foam is its density and so tests have been carried out over a range of foam densities from 32 to 360 kg/m³.

FRACTURE TESTS

Single edge notch fracture tests were carried out as described previously⁴. It has been shown that a low density rigid polyurethane foam obeys the Griffith criteria for fracture in so far as the predicted behaviour of tensile strength on the size of artificially introduced cracks is concerned. In this study the previous work has been extended by the use of l.e.f.m. to characterize the fracture behaviour.

Irwin⁵ is attributed with introducing the elasticity solution for the energy release rate, G , and also the concept of K , the stress intensity factor. For an infinite plate in plane stress G is given by

$$G = \frac{\sigma_m^2 \pi a}{E} \quad (1)$$

where σ_m is the applied stress; $2a$ is the crack length; E is the modulus. For plane strain conditions $E/(1 - \nu^2)$ should be used where ν is Poisson's ratio.

The stress intensity factor K is given by

$$K = \sigma \sqrt{\pi a} \quad (2)$$

Irwin⁵ also showed that there is a relationship between K and G namely:

$$K^2 = EG \quad (3)$$

The single edge notch (s.e.n.) specimens tested were clamped using fixed grips with the result that bending of the specimens was restrained. Harris⁶ has obtained results for an edge crack in a sheet which does not bend giving the result

$$\frac{K_{Ic}}{\sqrt{\pi a}} = \sigma Y \quad (4)$$

where Y is equal to

$$Y = \frac{5}{(20 - 13(a/W) - 7(a/W)^2)^{1/2}}$$

a being the crack length and W the specimen width. Therefore a plot of σY versus $1/\sqrt{\pi a}$ will give a straight line graph of slope equal to K_{Ic} (critical stress intensity factor). Values of K_{Ic} were calculated by plotting graphs of σY versus $1/\sqrt{\pi a}$.

PREPARATION OF POLYURETHANE FOAMS

Rigid polyurethane foams were prepared from a commercial two component system, Propocon MR49 and Isocon M supplied by 'Lankro Chemicals Ltd' (see appendix for the ingredients of the foam system). The manufacturer's recommendation being that the two components be mixed on a 1:1 weight ratio.

Foams of low density i.e. 32 kg/m³ were prepared by mixing the above components with a high speed mixer, the foam mixture obtained being poured into an open mould and allowed to rise freely. For higher density foams an enclosed mould of dimensions 15 × 11 × 3.7 cm was used to fabricate blocks of foam. The mould was constructed such that one or all of the walls could be removed from the completed foam block by releasing corner brackets which held the walls together. To facilitate removal of the blocks from the mould the walls were coated with a thin film of petroleum jelly, and constraint of the foam within the mould was

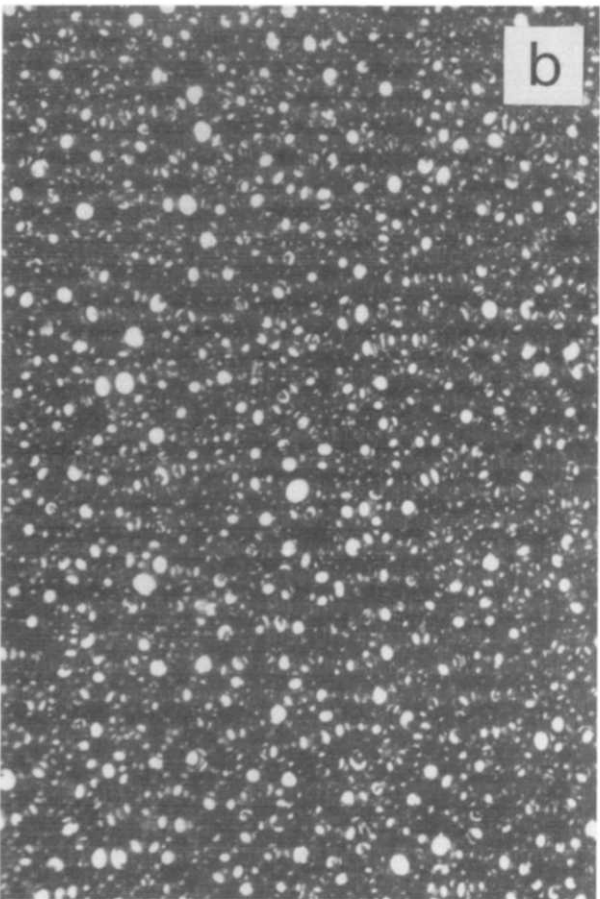
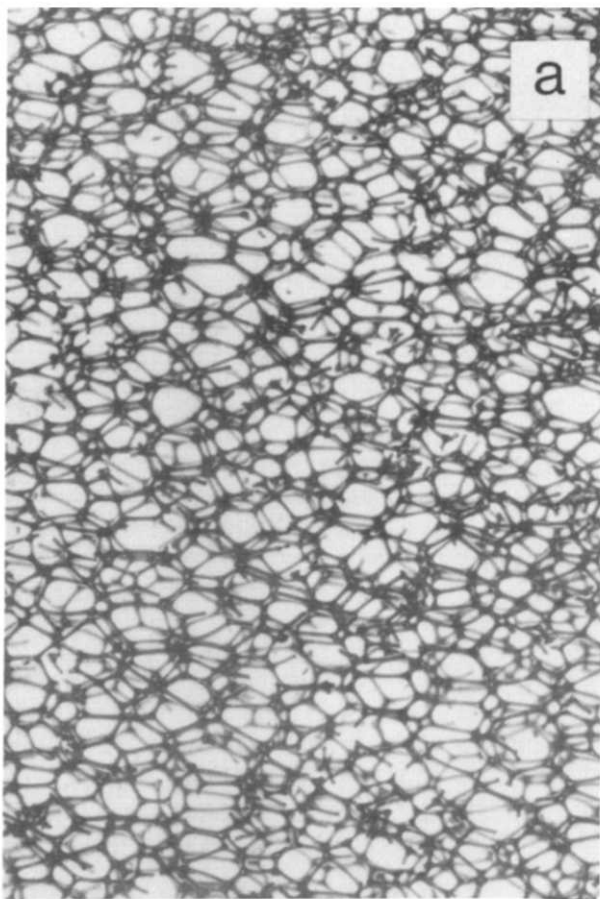


Figure 1 Photographs of microtomed foam specimens (a) foam of density 35 kg/m³, magnification 10X, (b) foam of density 185 kg/m³, magnification 10X

achieved by the use of top and bottom plates which were clamped securely.

To fabricate foams of density 200 kg/m³ and upwards the amount of blowing agent and catalyst was reduced to allow enough time for adequate mixing and filling of the mould prior to rise of the foam. The pressures needed to constrain the foam within the mould were high so that after filling the mould was placed in a small hydraulic press.

FOAM MORPHOLOGY

The physical structure of a foam is an important parameter affecting the physical properties of the material. Figure 1 shows photographs of microtomed foam specimens illustrating how the cell structure of the foam alters with density. It can be clearly observed that polyhedral morphology predominates at low densities (Figure 1a). These foams are characterized by relatively thin cell walls extending between thicker struts. Figure 1b shows that at higher densities the polyhedral morphology changes to a structure of isolated spheres set in a polymer matrix.

Methods of measuring the proportion of closed cells in a rigid foam are based on the measurement of the volumetric displacement of either liquid or gas by the foam. The closed cell content of foam specimens was determined using ASTM Test Method D1940-62T which is an adaption of that of Remington and Pariser⁷. This showed that the foams were predominantly of a closed cell nature. Foam densities were determined by using ASTM Test Method D1622 which simply involves measuring the dimensions of a block of foam and then weighing.

To investigate foam morphology and in particular obtain a measurement of cell size a photographic technique was employed for foams up to density 180 kg/m³. This involved the microtoming of foam samples to give thin sections which were of the order of two to three cells thick. Transmitted light from a photographic enlarger was passed through the microtomed specimens onto photographic film (Kodak Tri X Ortho Film). The exposed film when developed could be enlarged to any desired magnification and prints could be taken to give a permanent record. Measurements of cell size were made from the magnified photographs (magnifications between 60 to 80 times were used depending on foam density) by measuring the diameters of a large number of cells i.e. at least 50 cells. For foam of higher density cell sizes were measured with a Reichert microscope using magnifications between 100 and 120 times, and measuring cell diameters with a graticule eyepiece.

RESULTS

Values of K_{Ic} have been obtained by using equation (4). Graphs of σY versus $1/\sqrt{\pi a}$ were plotted and values of K_{Ic} were calculated from the gradients. Such a plot is illustrated in Figure 2 which is a graph of σY versus $1/\sqrt{\pi a}$ for a foam having a density of 120 kg/m³. Figure 3 shows a graph of the K_{Ic} values found in this way versus foam density (ρ).

Figure 4 is a graph of G_{Ic} (the critical strain energy release rate) versus foam density, values for G_{Ic} at different foam densities being determined using the relationship

$$G_{Ic} = \frac{K_{Ic}^2}{E}$$

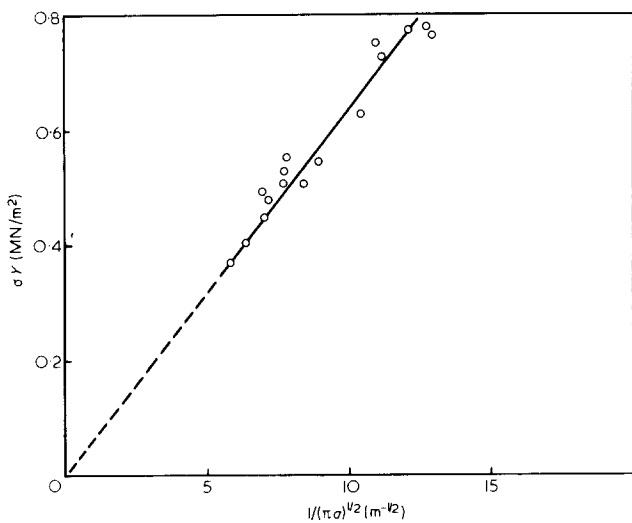


Figure 2 Graph of αY versus $1/\sqrt{\pi a}$ for foam of density 120 kg/m^3

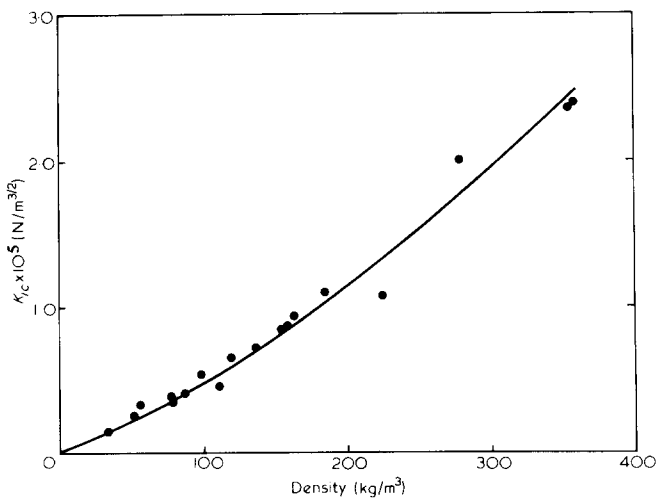


Figure 3 K_{Ic} versus density

(see equation 3). Modulus values have been determined from tension tests using a strain rate corresponding to the strain rate used in testing the s.e.n. specimens. Figure 4 shows that G_{Ic} passes through a minimum as foam density increases.

Another parameter, namely crack opening displacement has been used by other workers⁸ to characterize the fracture of solid polymers and in the present work the value of this parameter has also been investigated. Crack opening displacement for propagation of a crack may be written as:

$$\delta = \frac{K_{Ic}^2}{E\sigma_y} \quad (5)$$

The localized yield stresses σ_y at the crack tip is a difficult parameter to determine but if it is assumed that to a first approximation $\sigma_y = E\epsilon_y$ then equation (5) can be rewritten as

$$\delta = \frac{K_{Ic}^2}{E^2\epsilon_y} \quad (6)$$

For a foam the tip of a crack must terminate at a cell and so the unstrained crack tip diameter should be the cell size c . As

the foam is strained the crack tip diameter will increase until a critical crack opening displacement is reached and failure occurs. At this point a failure strain for the cell wall at the crack tip may be defined by

$$\epsilon_f = \frac{\delta}{c} = \frac{K_{Ic}^2}{\epsilon_y E^2 c} \quad (7)$$

where c is the cell diameter of the foam.

Figure 5 is a graph of crack opening displacement versus density, the values of c.o.d. having been calculated from equation 6. It can be seen that at low densities c.o.d. is high but as density is increased the c.o.d. falls rapidly and decreases slowly at high densities.

Using equation 7 values for failure strain ϵ_f at the crack tip have been calculated and the results are shown plotted against density in Figure 6. In calculating ϵ_f , values of ϵ_y , the macroscopic yield strain were determined from compression tests carried out using a strain rate corresponding to that used in the s.e.n. fracture tests. The yield point in compression is well defined for both low and high density foams. For low density foam the yield point is indicated by a drop in load while at high density a point of inflexion occurs. In tension the yield point is much less clearly defined as can be seen from Figure 14 which shows stress/strain

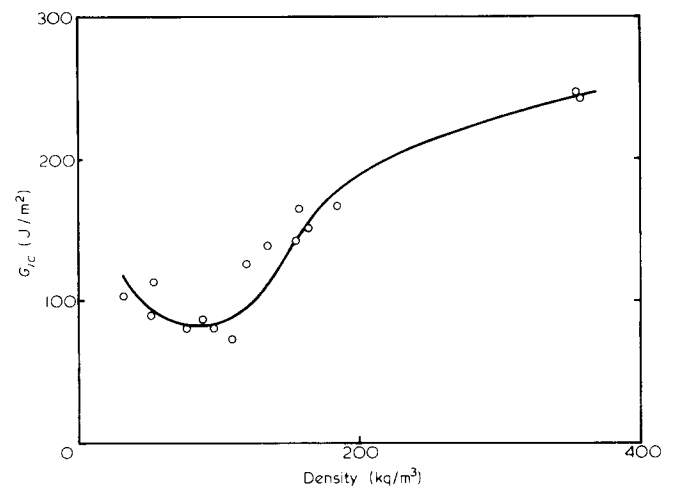


Figure 4 G_{Ic} versus density

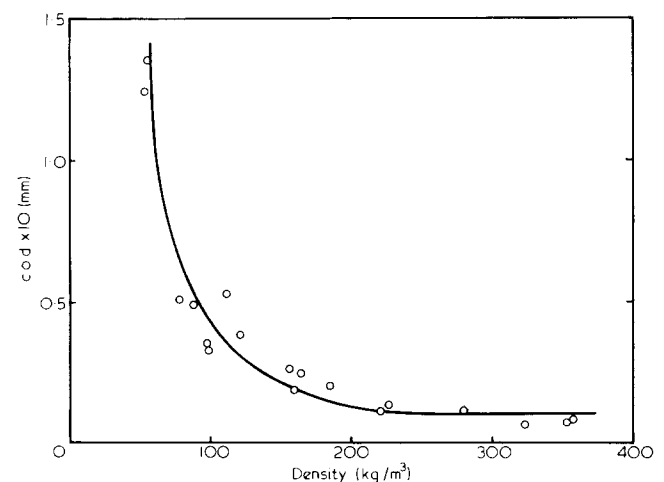


Figure 5 Variation of crack opening displacement with density

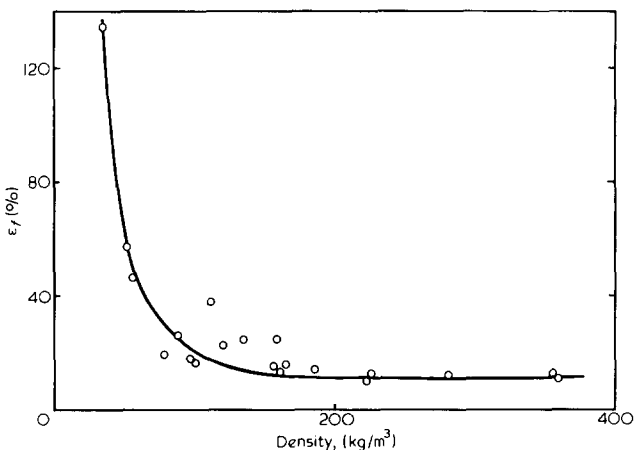


Figure 6 Microscopic percentage failure strain at the crack tip versus density

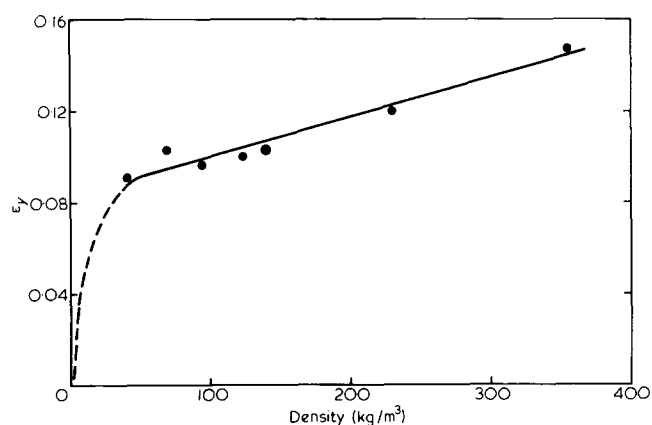


Figure 7 Graph of yield strain versus density

curves for low and high density foams. Figure 7 is a graph of ϵ_y versus density and values of ϵ_y which were used in the calculation of failure strain were taken from this line. It can be seen from Figure 6 that after an initial steep drop the failure strain remains sensibly constant above the foam density of 120 to 130 kg/m^3 , and takes a value of 12%. Figure 8 shows a plot of percentage failure strain for unnotched specimens determined from tensile tests carried out on a Hounsfield Type E testing machine using the plastics extensometer. It can be seen from the graph that a similar type of behaviour occurs on the macroscopic scale as on the microscopic scale at the crack tip. As density increases there is an initial rapid drop in the failure strain which then levels out to a constant value, the value in this case being approximately 4%.

DISCUSSION OF RESULTS

As might be expected values of the critical stress intensity factor K_{Ic} increase with increasing density indicating increased toughness with increase in density. Values of G_{Ic} (the critical strain energy release rate) are shown in Figure 4 and contrast with K_{Ic} values in that a minimum appears in this graph at a density of approximately 100 to 110 kg/m^3 , which corresponds to the density region in which the morphology of the foams change. At densities below 100 to 110 kg/m^3 , the foams have a polyhedral type structure

(Figure 1a) whilst at densities above 110 kg/m^3 the cells of the foam take on a spherical structure (Figure 1b). G_{Ic} has been calculated from equation (3) so that G_{Ic} is a function of both K_{Ic} and E both of which are in turn functions of density (see Figures 3 and 9). The slope of the G_{Ic} versus density curve is hence dependent on the relative rates of increase of K_{Ic} and E with density. It is generally accepted that the crack tip stress or strain field cannot be characterized by a single parameter when yielding in the crack tip becomes extensive. However the amount of crack opening prior to crack extension may be used as a parameter which is characteristic of the crack tip region. Values of c.o.d. (δ), calculated from equation 6, are shown in Figure 5 from which it is possible to calculate values for failure strain ϵ_f using equation 7. Figure 6 shows that after an initial drop the values of ϵ_f become sensibly constant. It is proposed that in the region in which ϵ_f is constant the mechanism of failure is by straining to break the ligament or ligaments ahead of the crack tip. A diagrammatic representation of such a mechanism is shown in Figure 10. The ligament a immediately ahead of the crack tip will be strained to breaking

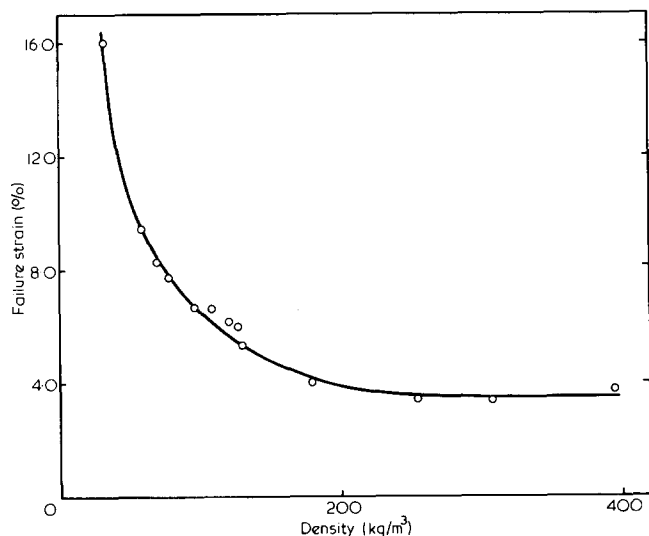


Figure 8 Graph of percentage failure strain versus density for unnotched material

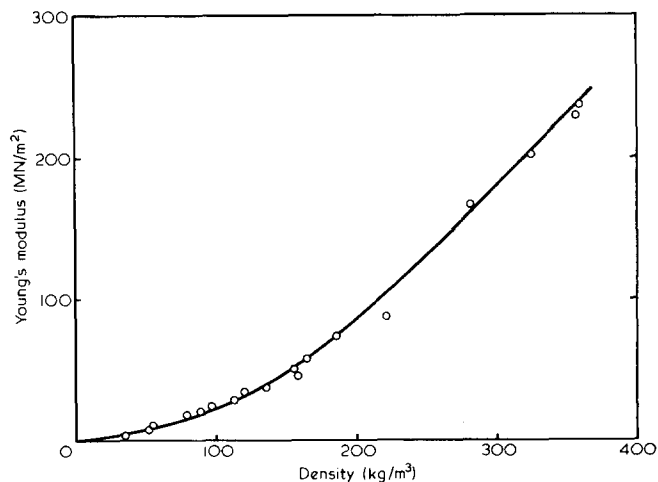


Figure 9 Graph of Young's Modulus (E) versus density

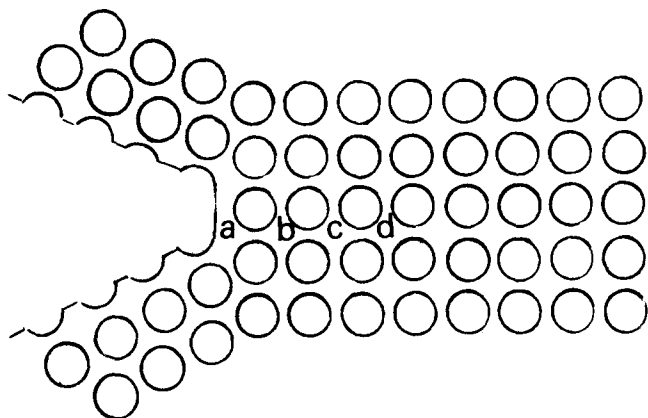


Figure 10 Failure mechanism of high density foam

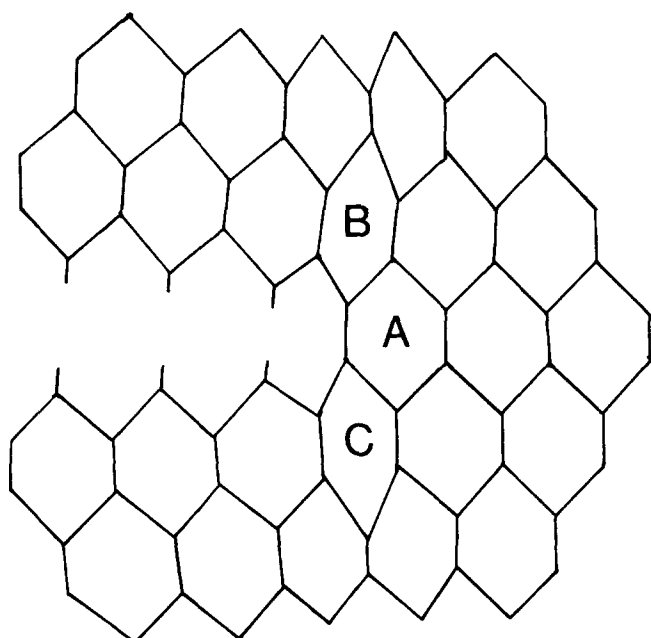


Figure 11 Failure mechanism of low density foam

point and the crack will advance by a similar mechanism through ligaments *b, c, d* etc.

Below a density of about 100 kg/m^3 the values of ϵ_f increase rapidly with decreasing density. At around this density the foam morphology changes from a spherical to a polyhedral structure and it is thought that the increasing failure strain may be a result of distortion of cells in the neighbourhood of the crack tip. The system is illustrated diagrammatically in *Figure 11*. In addition to the ligament between cell *A* and the crack tip being strained to break the failure strain may be increased by the deformation of cells such as *B* and *C* etc. Such deformation would be a result of bending or buckling of cell walls which are oriented obliquely to the direction of propagation of the crack. *Figure 12* is a photograph of a foam of density 35 kg/m^3 showing a cell labelled *A* deformed in this way, the crack tip is indicated by the arrow. That buckling or bending of cell walls can occur is also indicated by *Figure 8* which is a graph of failure strain for unnotched material versus foam density. At low densities failure strain is high indicating that deformation of cells may be occurring whilst at high densities the failure strain is much lower and constant.

An hypothesis that the above type of deformation occurs at low densities is also supported by consideration of changes

in the yield strength of the foam as a function of density *Figure 13*.

At low densities the yield stress, σ_y , is less than the tensile strength σ_T but at higher densities ($>125 \text{ kg/m}^3$) the curves cross and σ_y is greater than σ_T . It would therefore appear that at low density the foam would yield before failure occurred, whereas at the higher densities the material would fail without prior yielding. It must be noted that the yield strength results were obtained from compression tests where-



Figure 12 Photograph of cell deformed at crack tip of a foam of density 35 kg/m^3

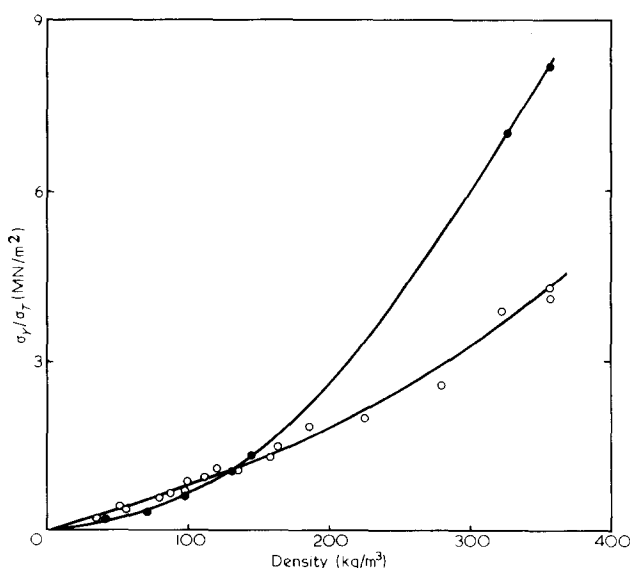


Figure 13 Graph of σ_y (●) and σ_T (○) versus density

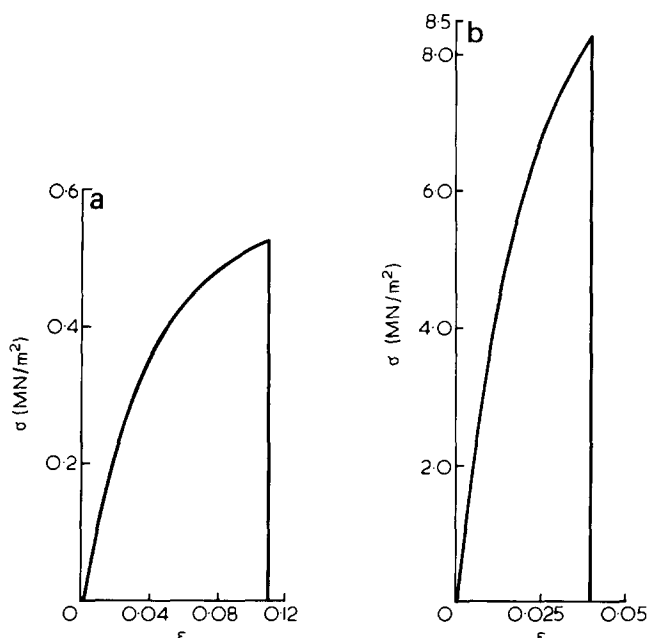


Figure 14 Stress/strain curves for (a) low density foam, (b) high density foam

as the conditions at the crack tip would essentially involve yield in tension. However the fact that the crossover in the σ_y/σ_T curves occurs at about the same density as the failure strain departs from a constant value seems significant, particularly when one considers that the morphology of the foam changes at about the same density. In addition if the tensile stress/strain traces for low and high density foam are examined it can be seen that there is a marked difference in behaviour (Figure 14). High density foam behaves essentially as a linear elastic material (Figure 14b), whereas the stress/strain trace for low density foam shows a marked non-linearity (Figure 14a). Nevertheless even at low densities plots of stress versus $1/\sqrt{\pi a}$ give reasonable straight lines from which values of K_{Ic} may be evaluated. At high density, examination of the fracture surfaces of the foams leads one to classify the fracture process as essentially brittle since the fracture surfaces show only minor irregularities and the surfaces are nominally flat. At low density however the fracture surface is quite irregular, and although the specimens show little evidence of gross yielding or necking, tensile specimens fail obliquely to the stretch direction indicating ductile failure. Throughout the density ranges covered the s.e.n. specimens failed catastrophically indicating unstable fracture rather than slow crack growth. At present work is continuing to verify this mode of failure using double cantilever beam specimens.

A characteristic inherent flaw size of a foam can be determined from the relationship

$$a' = \frac{1}{(1.12)^2 \pi} \left(\frac{K_{Ic}^2}{\sigma_T^2} \right)$$

where a' is the flaw size and σ_T is the tensile strength of unnotched material. It is not unreasonable to assume that the inherent flaw size of a foam may have the dimensions of the cell diameter of the foam. The inherent flaw size was found to be greater than the average cell diameter (see Table 1) but approximated to the size of the largest voids which were observed in the foam. These voids are not actual cells but are air inclusions caused by air entrainment in the mixing stage

of foam formation. Figure 15 shows calculated characteristic void sizes and measured void sizes. Other workers⁹⁻¹¹ have obtained similar relationships between measured and observed void sizes of foamed materials.

CONCLUSIONS

The data obtained indicates that the strength of rigid polyurethane foam may be characterized by the parameters G_{Ic} , K_{Ic} and crack opening displacement. The use of c.o.d. is of particular interest since the parameter ϵ_f which is derived from it (equation 7) becomes sensibly constant above a foam density of approximately 130 kg/m^3 . In equation (7) the parameters ϵ_y , E and c are relatively easily determinable quantities. If ϵ_f is determined from fracture tests on a single high density foam for a particular urethane foam system then the fracture toughness K_{Ic} for foams of other densities may be calculated.

Table 1

Foam density (kg/m^3)	Mean cell diameter (mm)
35	0.384
55	0.290
79	0.263
88	0.188
97	0.195
99	0.183
112	0.144
120	0.164
135	0.142
155	0.170
158	0.136
160	0.130
164	0.150
185	0.142
222	0.104
225	0.099
280	0.092
322	0.081
356	0.061
358	0.058

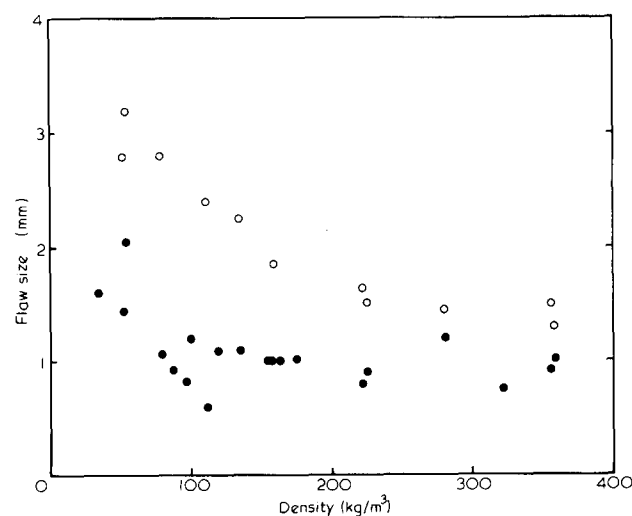


Figure 15 Experimental flow size (○) and theoretical flow size (●) versus density

It is also interesting to note that whilst K_{Ic} increases continuously with increasing foam density the parameters c.o.d. and ϵ_f behave rather differently. At low densities these parameters take high values characteristic of the ductile mode of failure of the polyhedral structured foams but as density increases their values fall. When the density of the foam is such that a spherical structure exists the values of c.o.d. and to a greater extent ϵ_f remain virtually constant as density increases.

ACKNOWLEDGEMENTS

The authors would like to thank Dr G. P. Marshall of the Department of Polymer Technology, Manchester Polytechnic, for many useful discussions on the subject of fracture mechanics during the course of the work.

REFERENCES

- 1 Marshall, G. P., Coutts, L. H. and Williams, J. G. *J. Mater. Sci.* 1974, **9**, 1409
- 2 Parvin, M. and Williams, J. G. *Int. J. Fract.* 1975, **11**, 963
- 3 Parvin, M. and Williams, J. G. *J. Mater. Sci.* 1975, **10**, 1883
- 4 Anderton, G. E. *J. Appl. Polym. Sci.* 1975, **19**, 3355
- 5 Irwin, G. R. 'Fracturing of Metals', Am. Soc. Metals, Cleveland, 1948
- 6 Harris, D. O. *J. Bas. Engng.* 1967, **89**, 49
- 7 Remington, W. J. and Pariser, R. *Rubber World* 1958, **136**, 261

- 8 Ferguson, R. J., Marshall, G. P. and Williams, J. G. *Polymer* 1973, **14**, 451
- 9 Fowlkes, C. W. *Int. J. Fract.* 1974, **10**, 99
- 10 Gent, A. N. and Thomas, A. G. *J. Appl. Polym. Sci.* 1959, **11(b)**, 354
- 11 Whittaker, R. E. *J. Appl. Polym. Sci.* 1974, **18**, 2353

APPENDIX

The formulation of the Propocon MR49/Isocon M foam system is:

Propocon MR49

	(Parts by weight)
R.F.55	65 (sorbitol)
D402	35 (low molecular weight diol)
Propamine D	2.6 (tetramethyl ethylene diamine—catalyst)
Water	1.3
Freon II	25.0 (trichlorofluoromethane—blowing agent)
Silicon surfactant	1% (based on weight of polyol)

Isocon M is a crude mixture of diphenyl methane diisocyanate (m.d.i.) which typically contains about 55% diphenyl methane diisocyanates (4,4'- and 2,4'-isomers), 25% triisocyanates and 20% higher polyisocyanates.